Contrib Mineral Petrol (1993) 113:185–195

Contributions to Mineralogy and Petrology

Diverse metal sources of Archaean gold deposits: evidence from in situ lead-isotope analysis of individual grains of galena and altaite in the Ross and Kirkland Lake deposits, Abitibi Greenstone belt, Canada

Keiko Hattori

Ottawa-Carleton Geoscience Centre, and Department of Geology, The University of Ottawa, Ottawa, K1N 6N5, Canada

Received June 15, 1992 / Accepted October 7, 1992

Abstract. Lead isotope compositions for individual grains of galena and altaite (PbTe) were determined in situ using a secondary ion mass spectrometer (SIMS). Galena was collected from the Ross deposit and altaite from the Kirkland Lake (KL) deposits in the southern Abitibi greenstone belt, Superior Province of Canada. The samples from KL are more radiogenic than those from the Ross deposit. Isotopic compositions vary significantly between different grains in each deposit and form broad linear arrays in $^{207}Pb/^{204}Pb$-$^{206}Pb/^{204}Pb$ and $^{208}Pb/^{204}Pb$-$^{206}Pb/^{204}Pb$ diagrams. The linear arrays of Pb-isotope data are attributed to mixing of Pb from different sources. At least two sources are required for individual deposits: one with low U/Pb and Th/Pb ratios and the other with high ratios. Lead minerals occurring with Au are less radiogenic than those that are not obviously associated with Au, suggesting that Au was supplied from low U/Pb sources, such as sulphides or older ultramafic-mafic rocks. While most data are consistent with the derivation from local rocks, highly radiogenic Pb with relatively low $^{207}Pb/^{206}Pb$ ratios recorded at KL require post-Archaean mineralization or derivation of the Pb from an unusual crustal source with low μ. The latter interpretation is favored because of the lack of textural evidence and because it is difficult to dissolve and precipitate altaite at low temperatures. The presence of a Pb reservoir with low μ is also inferred from the data of Archaean banded iron formations and volcanogenic massive sulphide deposits. Different isotopic patterns of the two deposits suggest different sources of metals in the two deposits. While this conclusion does not reject the derivation of fluids from the lower crust or mantle, the data are not in accord with conceptual models invoking a common source reservoir for metals. The study suggests that fluids, which may have a common origin, leached metals and other constituents from the upper crustal rocks during their ascent. The proposed model, different origins for different constituents, explains much of the conflicting evidence presented by Archaean Au deposits, including provinciality of mineralogy and relatively uniform fluid inclusion and C-isotope data from many Au deposits.

Introduction

Lead-isotopic data from metallic deposits have been used to identify sources of metals and to constrain genetic models of their mineralization. For Au deposits, previous Pb-isotope studies have shown significant isotopic variations compared with volcanogenic massive sulphide deposits (Thorpe 1982; Franklin et al. 1983; Thorpe et al. 1984). Causes for this variation may be more apparent on the microscale. Thus, in this study, the Pb-isotope compositions of individual grains of Pb minerals from gold-bearing veins were determined by secondary ion mass spectrometer (SIMS).

SIMS has been a powerful tool for examining intra- and intergrain variations of isotopic ratios and trace elements (Hart et al. 1983; McKibben and Eldridge 1990). This paper presents the results of in situ isotopic analyses of galena and altaite from the Ross and KL deposits in the southern Abitibi greenstone belt of the Superior Province of Canada. These deposits were selected because they show vein textures and mineralogy similar to many other Archaean Au deposits and because their geological setting and mineralization have been well studied. Also, the KL Au deposits are known to contain unusually high radiogenic Pb, whereas galena samples from the Ross deposit are non-radiogenic, similar to most other Archaean Au deposits (Thorpe 1982).

Geology and mineralization

The Kirkland Lake camp has produced more than 910 tons of Au, which makes it the second largest Archaean Au camp in North America (Ploeger and Crocket 1982). The "camp" is divided into several mine properties, forming a series of deposits along a splay of the Larder Lake-Cadillac Fault (LLCF). The Ross deposit, which has yielded ~30 ton of Au since 1984 (Akande 1982), is located on a splay off the Destor-Porcupine Fault (DPF) (Fig. 1). Both LLCF and DPF are east-trending dextral shear zones and significant Au camps in the Abitibi belt are all located along these two major deformation zones, including the Porcupine-Timmins, Harker-Holloway, Matachewan, Larder Lake, Rouyn-Noranda, Bousquet, and Val d'Or camps. Sub-greenschist facies regional metamorphic grade (Jolly 1978), vein textures indicative of brittle

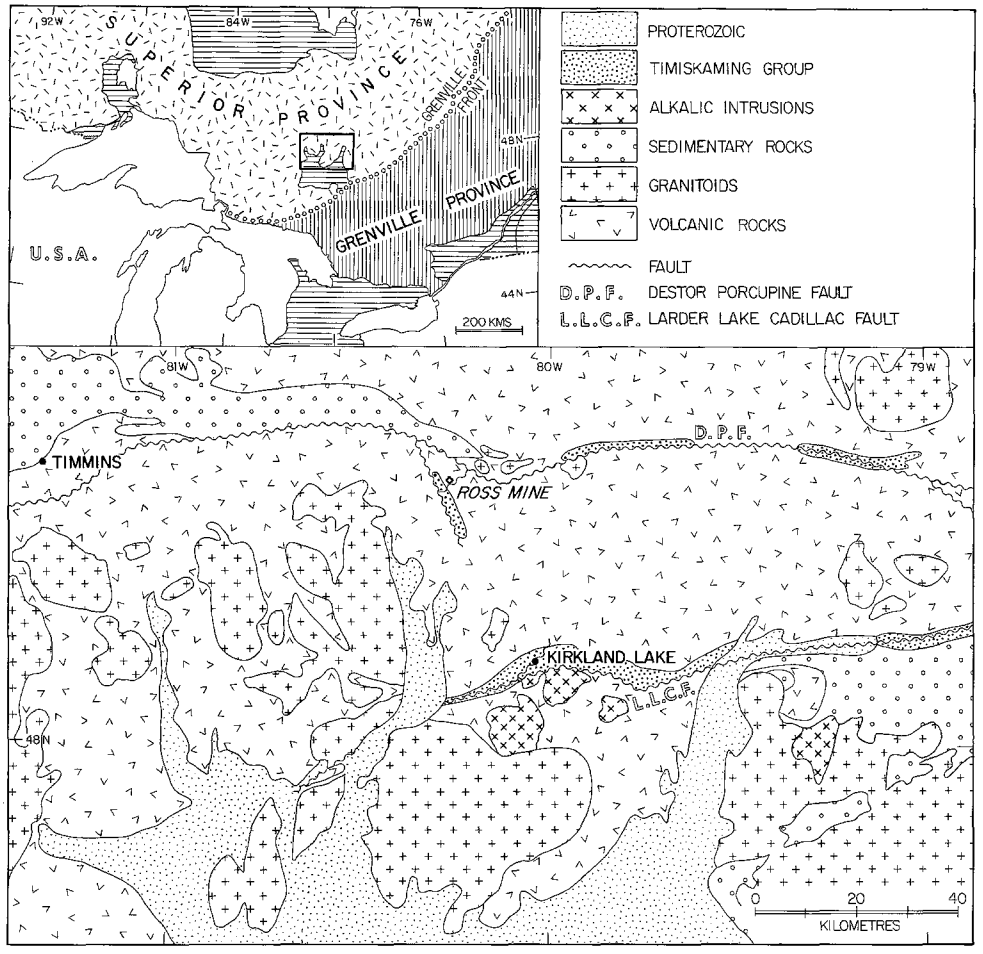

Fig. 1. Location of the KL and Ross deposits and geology of the study area in the Southern Abitibi Greenstone belt. The area shown in the lower diagram is indicated by the boxed regional diagram above. (Modified from OGS-MERQ, 1983)

failure, and alteration assemblages suggest that they represent deposits formed in shallow levels of the Archaean crusts (e.g. Colvine 1989).

Gold-bearing veins cut metamorphosed greenstones, and intrusions into the greenstones. The major intrusions are dated at 2680 at 2690 Ma (e.g. Corfu et al. 1989), but the exact age of the veining is still in debate. Attempts to date minerals from gold-bearing veins elsewhere in the Abitibi belt, including muscovite, rutile and scheelite, have given substantially younger dates, which include 2403 ± 47 Ma (Bell et al. 1989) and 2599 ± 7 Ma (Wong et al. 1991). However, there is no consensus on whether these dates represent the time when Au introduced. Young ages may reflect cryptic, later metamorphic events (e.g. Schandl and Gorton 1991). Various $^{40}Ar/^{39}Ar$ ages from a single deposit (e.g. Masliwec et al. 1985) suggest a long history of vein formation.

Kirkland Lake gold deposits

The greenstone rocks are mostly ultramafic to mafic rocks with ages ranging from 2705 ± 1 to 2701 ± 1 Ma (Corfu et al. 1989). These are overlain unconformably by sedimentary and volcanic rocks of the Timiskaming Group. Detailed U-Pb zircon studies suggest that the Timiskaming Group was formed at ~2680 Ma and that they were intruded by the alkalic to sub-alkalic intrusions of similar age (Corfu et al. 1991). The geology of the area and occurrences of the mineralization are described by Thomson et al. (1950), Hicks and Hattori (1988) and Hattori and Hodgson (1990).

The Au deposits are principally hosted by alkalic to subalkalic igneous rocks of the KL Intrusive Complex of the Timiskaming Group. The auriferous veins consist of greasy gray quartz and minor amounts of pyrite and carbonates. The early-formed quartz has been extensively recrystallized under ductile deformation at ~350° C (Hattori and Levesque 1989) and was fractured and cut by various late veinlets. They range in width from several centimeters to several micrometers and cross-cut each other; they contain clear quartz, sulphide, carbonates, quartz-carbonate, and sulphide-tellurides (Hattori and Levesque 1989). Different veinlets are common within a single polished section of 2.4 cm diameter.

Introduction of Au was late, as documented in other Archaean deposits. Most Au occurs in late fractures (Hattori and Levesque 1989) as native gold and Au tellurides (calaverite, $AuTe_2$, and petzite, Ag_3AuTe_2). Gold grains are commonly accompanied by tellurides: altaite (PbTe) and coloradoite (HgTe). Intergrowth of Au phases and tellurides suggests that some altaite grains formed together with Au (Fig. 2a).

Two samples used for isotopic analyses were collected in the Kirkland Lake Gold (THO-1) and Macassa (THO-2) properties in the central part of the KL camp. Both samples have dark quartz containing cross-cutting veinlets of sulphide (pyrite, chalcopyrite) and auriferous telluride minerals. Some pyrite grains were recrystallized to form cubes; other sulphides and altaite are enclosed in the cubes. Altaite is the main Pb phase in the deposits, and native gold amost always occurs together with altaite, which is anhedral and commonly elongated along the fractures. There is no textural evidence of overgrowth or zoning of the altaite grains.

Ross

Timiskaming Group sedimentary and volcanic rocks also occur along a splay of the DPF near the deposit (Fig. 1). The volcanic rocks are identical in chemical compositions (Hattori 1989) and U-Pb zircon ages (~2680 Ma; Corfu et al. 1991) to those of KL.

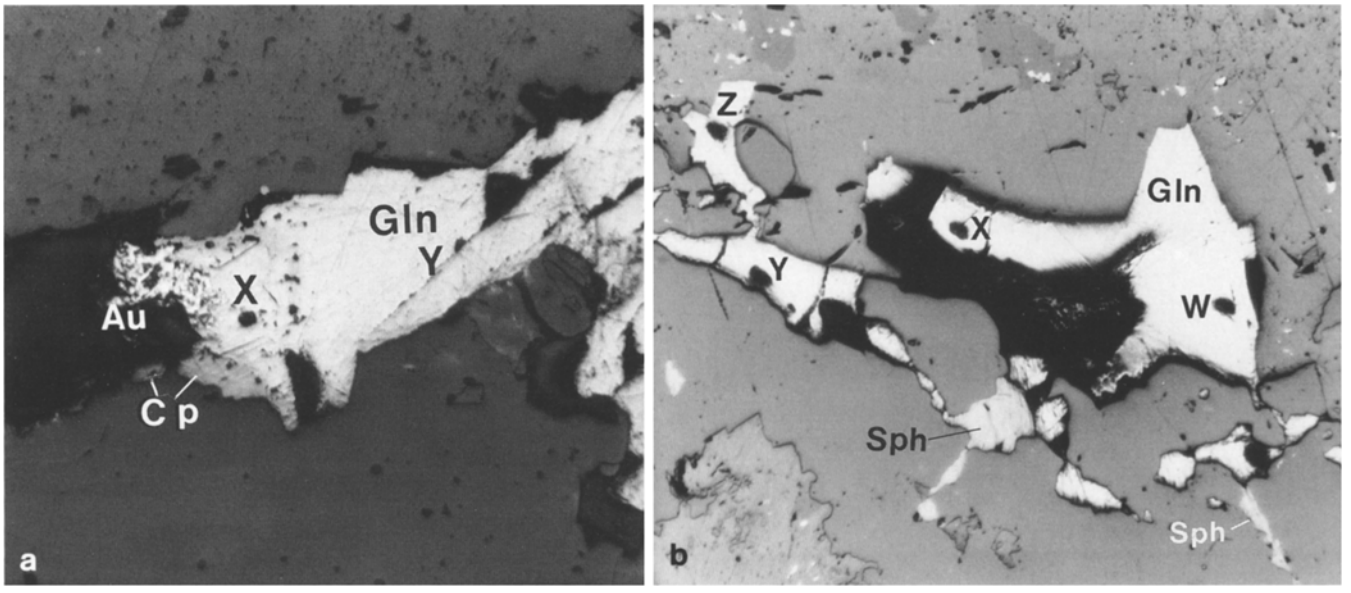

Fig. 2a, b. Photomicrographs showing two types of galena grains from the Ross deposit and SIMS analytical craters (W, X, Y, Z). **a** Galena (Gln) intergrown with native gold (Au) in the sample 84619-6. X and Y correspond to AA3 and AA2 in Table 1. Cp = chalcopyrite, Field of view = 0.35 mm. **b** Coarse galena (Gln) associated with sphalerite (Sph) in the sample, 89531-4. W, X, Y, and Z correspond to A1, A2, B and C in Table 1. Field of view = 0.73 mm

The geology of the area and the mineralization are described in Akande (1982) and Troop (1986). The Au deposit is hosted by basalts and andesites of the Stoughton-Rochemoure Group (2714 ± 2 Ma; Corfu et al. 1989) and minor porphyritic intrusions (Troop 1986). Similar porphyritic intrusions in Timmins have been dated at ~2690 Ma (Corfu et al. 1989). Similar geological settings of the KL and Ross areas suggest that the ages of mineralization may also be similar. Auriferous veins at Ross primarily consist of quartz and minor carbonates. Coarse base metal sulphides such as chalcopyrite, bornite, tetrahedrite, pyrite and galena are common. Gold occurs primarily as native gold. There are two types of galena: fine anhedral grains associated with Au and coarse cubes of galena in base metal-rich portions of the veins. A single section may contain veinlets of different mineralogy and different types of galena.

Samples for this study came from sulphide-rich portions of quartz veins (veins 12 and 13–14). Sample 890531-4 represents the coarse base-metal-rich portion (sphalerite, galena, pyrite and chalcopyrite) and no native gold was detected in the sample. Sample 890531-8 contains chalcopyrite, galena, pyrite, and a small native gold grain (~10 μm). Sample 840619-6 consists of quartz containing veinlets of auriferous base metal and non-auriferous coarse base-metal sulphides.

Analytical methods

Lead isotopic compositions were determined on galena and altaite grains in polished sections coated with Au, using the MIT-Havard-Brown Cameca IMS 3f ion microprobe. No mineral separation or concentration procedures were undertaken before several rock chips were mounted in Al rings filled with an Epoxy resin. The sections were polished manually on cloth using diamond and Al_2O_3 abrasives. Typical grains used for the analysis are shown in Fig. 2a and b.

Operating conditions were essentially the same as those described in Hart et al. (1983). A beam of O^- with ~50 nA current was focused to a diameter of 20 to 30 μm. The beam was directed to the area selected for analysis for ~5 min before each data acquisition, which burned off the Au coating and surface layers high in Hg and other contaminants. Atomic masses 202 and 203 were checked for the presence of Hg and Tl before commencing data acquisition because of isobaric interference of ^{204}Hg and ^{203}Tl-hydride on the peak of ^{204}Pb. This procedure was important because coloradoite (HgTe) and native gold grains contain Hg and because Tl contents are high in some Archaean Au deposits (Cameron and Hattori 1985). Peak intensities of the masses of 204, 206, 207 and 208 were determined successively by changing the magnetic field intensity (a single cycle). Seven cycles of measurements were obtained for a block and six sets of doubly time-interpolated ratios were calculated and 5 to 7 blocks of data were obtained for a single spot analysis. A single analysis took an average of ~50 min.

For isotopic analysis of grains adjacent to native gold, the 202 peak was also collected to make sure that the 204 peak was not enhanced by Hg. Analytical precision (2σ) of the mass ratio measurements for both 207/206 and 208/206 is normally < 0.05%.

Measured Pb-isotope ratios were corrected for instrumental mass fractionation and for hydrides. Correction for hydrides was negligible (< 0.01%), as determined by comparing peak intensities of mass 208 and 209 (^{208}PbH). Corrections for mass fractionation were obtained by measuring the mass ratios of working standards, F-19 galena and KH-Al altaite. The galena standard, F-19, came from the Edward-Balmat deposit, and the ^{208}Pb/^{206}Pb and ^{207}Pb/^{206}Pb ratios are 2.1582 and 0.91543, respectively (Macfarlane 1989). The altaite standard, KH-Al, was from the Mattagami Lake deposit, which was donated by the Royal Ontario Museum (ROM-M-325556). The ratios of ^{208}Pb/^{206}Pb and ^{207}Pb/^{206}Pb were determined to be 2.5148 and 1.0920, respectively. The Pb-isotopic ratios were determined using a thermal ionization mass spectrometer after the dissolution of a small quantity of the sample in hot, double-distilled nitric acid (6.2 N). The isotopic homogeneity of the altaite standard was checked using the ion microprobe.

The standards were analyzed every 12 h and the data were normalized accordingly. The intrumental mass fractionations varied from 0.25 to 0.35% per atom mass unit for the galena standard, and from 0.05 to 0.18% per atom mass unit for the altaite standard, during the 10-month period of this study. The variations of the fractionations within any single period of analysis (24 to 48 h) were much smaller. Actual samples may contain small quantities of Te or S. The small difference of instrumental mass fractionation between the two Pb minerals made it unnecessary to calibrate mass fractionation for individual samples. Replicate measurements of

Table 1. Pb isotope compositions of galena and altaite determined by SIMS

Analysis[a] point	$^{206}Pb/^{204}Pb$	$^{207}Pb/^{204}Pb$	$^{208}Pb/^{204}Pb$	$^{208}Pb/^{206}Pb$	$^{207}Pb/^{206}Pb$	Remarks[b]
89531-4, Ross, Gln						
A1	13.355	14.468	33.074	2.476	1.083	r of lrg Gln grain, "A". W in Fig. 2b.
A2	13.396	14.502	33.307	2.486	1.083	Other r of the Gln grain, "A". X in Fig. 2b.
B	13.400	14.496	33.205	2.478	1.082	c of adj. Gln grain, "B". Y in Fig. 2b.
C	13.385	14.498	33.235	2.483	1.083	r of the grain attached to "B". Z in Fig. 2b.
D	13.392	14.493	33.253	2.483	1.082	Subhedral Gln
E1	13.449	14.537	33.328	2.478	1.081	r of lrg Gln, "D"
E2	13.397	14.496	33.220	2.479	1.082	other r of the grain, "D"
F	13.392	14.501	33.254	2.483	1.083	c of the grain
G	13.385	14.475	33.207	2.481	1.081	c of subhedral Gln
H	13.386	14.477	33.206	2.481	1.082	c of subhedral Gln
89531-8, Ross, Gln						
A1	13.224	14.415	32.961	2.492	1.090	r of Gln "A" adj. Sph.
A2	13.270	14.428	33.032	2.489	1.087	c of the gr "A".
A3	13.271	14.450	33.061	2.491	1.089	Near c of the gr "A"
B1	13.249	14.427	32.988	2.490	1.089	
B2	13.255	14.418	32.984	2.488	1.088	
C1	13.283	14.481	33.170	2.497	1.090	Gln "C" containing Sph incl., adj. Sph
C2	13.280	14.483	33.189	2.499	1.091	r of Gln "C" adj. Sph
C3	13.267	14.455	33.058	2.492	1.089	c of the gr "C"
C4	13.271	14.459	33.068	2.492	1.090	c of the gr "C"
D1	13.191	14.440	33.108	2.510	1.095	Adj. Au
D2	13.267	14.440	33.025	2.489	1.088	Adj. Au
84619-6, Ross, Gln						
DA1	13.273	14.449	33.041	2.489	1.089	Adj. Au
DB1	13.227	14.406	32.850	2.484	1.089	Fine gr in qtz
DA2	13.225	14.371	32.870	2.485	1.087	lrg subhedral Gln, enclosing Au, Cp
DA3	13.200	14.337	32.743	2.480	1.086	r of the gr
DA4	13.260	14.451	33.021	2.490	1.090	Adj. Au
DB2	13.184	14.310	32.908	2.496	1.085	in Qtz, near Au
DD	13.186	14.333	33.009	2.503	1.087	Small Gln encl. by Qtz
CC1	13.294	14.464	33.065	2.487	1.088	Gln-Sph veinlet
CA1	13.270	14.420	33.006	2.487	1.087	lrg Gln in Gln-Sph veinlet
CD1	13.279	14.449	33.034	2.488	1.088	Fine Gln in Qtz along Gln-Sph veinlet
CD2	13.329	14.482	33.147	2.487	1.087	Gln-Sph veinlet
CD3	13.259	14.402	32.937	2.484	1.086	Gln-Sph veinlet
DA5	13.235	14.372	32.838	2.481	1.086	r of the gr
DG1	13.196	14.313	32.657	2.475	1.085	Gln encl. in Sph
AA1	13.385	14.507	33.121	2.474	1.085	Coarse Gln, partially encl. by Au, in frac of Qtz
AA2	13.294	14.446	33.063	2.487	1.087	C of the gr, Y in Fig. 2a.
AA3	13.352	14.509	33.382	2.500	1.087	Adj. Au, X in Fig. 2a.
BA1	13.331	14.441	33.023	2.477	1.083	Sph-Gln aggr in Qtz
BA2	13.323	14.486	33.099	2.484	1.087	Sph-Gln aggr in Qtz
EA1	13.191	14.279	32.634	2.474	1.082	Gln-Au-Cp veinlet in Qtz, Fine Gln adjacent to Cp-Au mixture
EB1	13.195	14.314	32.610	2.471	1.085	Coarse Gln adj. Cp-Au mixture
EC1	13.163	14.288	32.581	2.475	1.085	Gln semi-encl. by a aggr of Cp-Au and Sph
EC2	13.160	14.280	32.580	2.476	1.085	c of the gr
CE	13.507	14.522	32.867	2.433	1.075	Sph-Gln veinlet
THO-2, Kirkland Lake, Alt						
DA1	14.488	14.889	33.834	2.335	1.028	
DA2	14.706	15.056	34.146	2.322	1.024	
DB	14.810	15.080	34.212	2.311	1.019	
DC	14.723	15.138	34.670	2.355	1.028	
DD	14.722	14.996	34.181	2.322	1.019	Encl. in pyrite
DE	14.955	15.257	34.584	2.313	1.020	
BA	14.533	14.860	33.850	2.329	1.022	Alt adj. lrg Au
BB	14.704	15.109	34.488	2.345	1.028	
BD	14.652	15.017	34.320	2.342	1.025	

Table 1 (continued)

Analysis[a] point	$^{206}Pb/^{204}Pb$	$^{207}Pb/^{204}Pb$	$^{208}Pb/^{204}Pb$	$^{208}Pb/^{206}Pb$	$^{207}Pb/^{206}Pb$	Remarks[b]
THO-1, Kirkland Lake, Alt						
AA	14.399	14.913	34.045	2.364	1.036	Alt adj. huge Au
AB1	14.364	14.876	33.961	2.364	1.036	Alt-Au veinlet
AB2	14.316	14.751	33.414	2.334	1.030	Au-Alt veinlet
BA	15.062	14.967	34.291	2.277	0.994	Cp-Py-Alt veinlet
BB	14.698	15.037	34.419	2.342	1.023	Adj. lrg Cp
BC	15.225	15.055	34.625	2.274	0.989	Cp-Alt veinlet in aggrs of Qtz
CA	15.489	15.102	34.854	2.250	0.975	Cp-Alt veinlet in frac of Qtz
CC1	15.765	15.081	34.789	2.207	0.957	Alt filling frac of Py
CC2	15.516	14.923	34.316	2.212	0.962	Alt filling frac of Py
CD	14.713	14.784	33.726	2.292	1.005	Alt encl. in Py
EA	14.354	14.889	33.831	2.357	1.037	Alt adj. Au
EB	14.364	14.889	33.855	2.357	1.037	
EC	14.761	14.927	34.213	2.318	1.011	Alt rimming pyrite
DA1	14.712	14.997	34.256	2.328	1.019	Au-Alt veinlet in frac of Qtz
DA2	14.854	14.983	34.245	2.305	1.009	Au-Alt veinlet in frac of Qtz
DB	14.905	14.957	34.217	2.296	1.004	Au-Alt veinlet in frac of Qtz

[a] Most sections contained several chips. When two letters appear in Analysis point, the first letter represents the label of chip and the second letter refers to Pb-bearing grain in the chip. Numbers after the letters indicate that multiple analyses were performed on a single grain

[b] Abbreviations: Adj. = adjacent to, Aggr = aggregate, c = centre of the grain, Encl = enclosed, Frac = fracture, gr = grain, lrg = larger, r = rim of the grain, Au = native gold, Alt = altaite, Cp = chalcopyrite, Gln = galena, Py = pyrite, Qtz = quartz, Sph = sphalerite

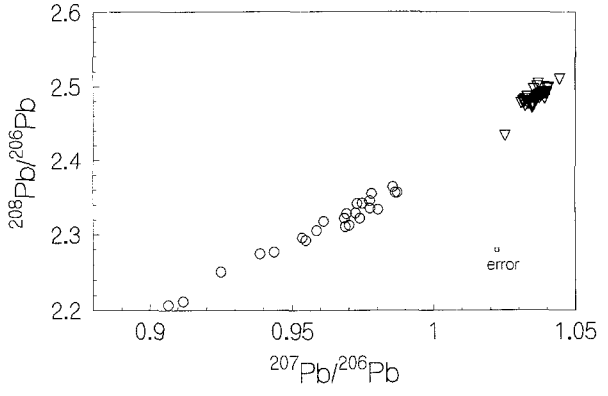

Fig. 3. Lead-isotopic compositions of galena from the Ross deposit (*inverted triangles*) and altaite from the KL deposit (*open circles*) determined by SIMS. Typical error range of individual analyses (2σ) is shown in the lower right corner (see details in Analytical method)

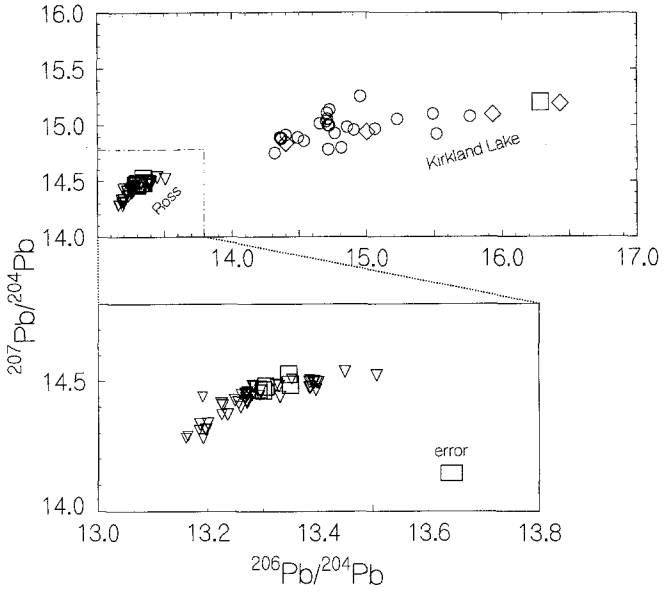

Fig. 4. Comparison of SIMS data and previously reported data. *Open circles*, SIM data from KL; *open diamonds*, reported values from the KL deposit (Sinclair 1982; Thorpe 1982); *inverted open triangles*, SIMS data of galena from Ross Mine; *open squares*, values of galena from Ross Mine reported by Thorpe (1982) and unpublished data by R.I. Thorpe. Legende as Fig. 3. Typical analytical error range (2σ) is shown in the *lower right*

the two standards suggest an overall reproducibility $\pm 0.2\%$. The error range of each ratio is, therefore, given as 0.2% because statistical counting errors are much smaller.

Results

The isotopic compositions are tabulated in Table 1. Intragrain isotopic variations and the presence of radiogenic rims were examined in several coarse grained samples. The SIMS study could not detect any isotopic variations (grains A and E of 890531-4; grains A and C of 890531-8). This is not surprising because there is no petrographic evidence of zoning or overgrowth.

Both the galena and the altaite samples show significant isotopic variations between grains from one locality. These isotopic variations are shown on a $^{207}Pb/^{206}Pb$ vs $^{208}Pb/^{206}Pb$ diagram (Fig. 3). Although this diagram does not convey geological meaning as well as the familiar $^{207}Pb/^{204}Pb$ vs $^{206}Pb/^{204}Pb$ diagrams, the plot validates the isotopic heterogeneity among the samples. Larger uncertainties are involved in the ratios of $^{207}Pb/$

^{204}Pb and $^{208}Pb/^{204}Pb$ than in the ratios without ^{204}Pb because the precise measurement of the least abundant ^{204}Pb is more difficult than that for the other isotopes. The spread of data in Fig. 3 confirms that the apparent isotopic variations are not due to analytical problems of ^{204}Pb.

Additional confirmation of the results is provided by Pb-isotopic compositions reported by other studies of the deposits determined by conventional analytical technique (Fig. 4). Reported $^{206}Pb/^{204}Pb$ ratios from the Ross deposit range from 13.29 to 13.35, with one exceptional value of 16.29 (Thorpe 1982). These values overlap the data obtained by SIMS in this study. Reported values from KL deposits (Thorpe 1982; Sinclair 1982) vary widely, but the variation is again comparable to the variation detected in two polished sections from these deposits (Fig. 4).

Ross deposit

Ratios of $^{206}Pb/^{204}Pb$, $^{207}Pb/^{204}Pb$, and $^{208}Pb/^{204}Pb$ for galena from the Ross deposit range from 13.16 to 13.51, from 14.28 to 14.54 and from 32.63 to 33.38, respectively. The data form a slightly curved array on a $^{206}Pb/^{204}Pb$-$^{207}Pb/^{204}Pb$ diagram (Fig. 5). Isotopic variations within individual sections (2.4 cm diameter) are relatively small (Table 1), but are considerably larger than the analytical uncertainties. Galena grains in contact with Au grains, or together with Au in the same veinlets tend to be less radiogenic than galena grains which are not in apparent association with Au, but values for the two types of galena overlap (Fig. 5). The former samples appear to define a steeper $^{207}Pb/^{206}Pb$ slope than galena that is not associated with Au (Fig. 5).

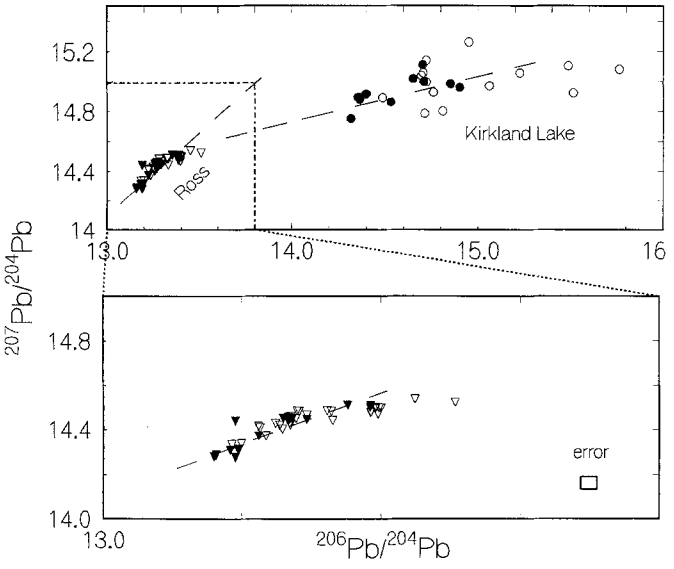

Fig. 5. Lead-isotopic compositions of galena and altaite. *Solid inverted triangles*, galena associated with Au in the Ross deposit; *open inverted triangles*, galena not associated with Au in the Ross deposit; *solid circles*, altaite spatially associated with Au at KL; *open circles*; altaite not associated with Au. Typical error range (2σ) is shown in the lower right corner

Kirkland Lake deposits

Altaite grains from KL are distinctly more radiogenic and show wider isotopic variations than galena grains from the Ross deposit. Data from Ross and KL form different clusters in the digrams (Figs. 3–5). The ratios of $^{206}Pb/^{204}Pb$, $^{207}Pb/^{204}Pb$ and $^{208}Pb/^{204}Pb$ for the KL samples vary from 14.31 to 15.76, from 14.75 to 15.26, and from 33.41 to 34.85, respectively. These isotopic variations were observed in individual sections (Table 1), and the values do not form well-defined linear arrays compared to those from the Ross deposit (Figs. 4 and 5). Altaite grains associated with Au are less radiogenic than those that are associated with chalcopyrite and pyrite (Fig. 5).

Discussion

Comparison with volcanogenic massive sulphide deposits

The isotopic heterogeneity observed in this study is in contrast with a narrow range of isotopic compositions observed from volcanogenic massive sulphide deposits (VMS) in Archaean greenstone belts (e.g. Thorpe et al. 1984). Archaean VMS occur in various rocks ranging from felsic to tholeiitic lithologies, and they are generally low in Pb (<0.1 wt %) compared to Phanerozoic Kuroko-type VMS. Despite the low concentrations and dispersed nature of Pb in the deposits, and various host rock lithologies, isotopic compositions of VMS are relatively homogeneous and the values are similar to crustal averages at the time of their formation (e.g. Doe and Stacey 1974). Different Pb isotopic signatures between VMS and Au deposits reflect different styles of hydrothermal activity for the two types of mineralization. Metals in VMS deposits were supplied from well-mixed sources, whereas metals in Au deposits were derived from diverse, poorly mixed sources.

Linear arrays of Pb isotope data

The slope of the isotopic data from the Ross deposit in Fig. 5, approximately coincides with the "^{204}Pb error line," which is due to uncertainty in the precise determination of ^{204}Pb signals. The possibility that the array reflects variation due to error is, however, rejected. First, isotopic variations in Ross are real as demonstrated in the $^{208}Pb/^{206}Pb$ vs $^{207}Pb/^{206}Pb$ diagram (Fig. 3). Second, the slope of the data from KL is quite different (Fig. 5). If the slope of the data from Ross is due to the analytical uncertainty of ^{204}Pb, the data from KL should also show a similar slope. Third, the slope of Ross data also coincides with the slope of all VMS deposits in the Abitibi greenstone belt (Fig. 6). The data from VMS were obtained by conventional high-precision mass spectrometers in many different laboratories; it is unlikely that this could be an artifact due to analytical uncertainty of ^{204}Pb. Instead, the data appear to indicate the presence of a Pb reservoir on the extension of the slope. The presence of such Pb reservoir is also inferred from the data from Archaean banded iron formations (BIF), described below.

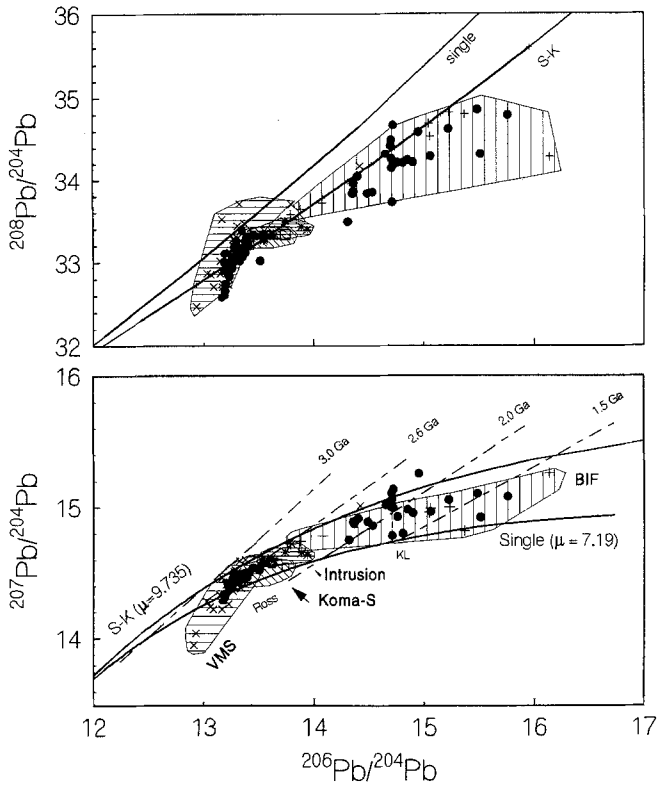

Fig. 6. Lead isotopic data of galena and altaite compared with various Pb reservoirs. *Solid circles*, this study. *Vertical-lined area* depicts BIF sulphides (leachates) in ~2.7 Ga banded iron formations in the southern Abitibi greenstone belt (Deloule et al. 1989); individual values are shown by the symbol, +. *Oblique-lined area* depicts Koma-S, sulphides in ~2.7 Ga komatiites, representing the values of late Archaean depleted mantle (Tilton 1983; Brévart et al. 1986; Dupré and Arndt 1990); individual values are shown by *open squares*. Note the heterogeneity. *Open horizontal-lined area* depicts VMS volcanogenic massive sulphide deposits of 2735 to 2700 Ma in the southern Abitibi greenstone belt (Tilton 1983; Franklin et al. 1983); individual values are shown by the symbol, X. *Close horizontal lined area*, late-kinematic intrusions in the southern Abitibi greenstone belt. Data for Preissac-Lacorne two mica granite (2630 to 2640 Ma, Feng and Kerrich 1991) are from Gariépy and Allègre (1985), those for Otto syenite stock (2680 ± 1 Ma, Corfu et al. 1991) are from Tilton and Kwon (1990); individual values are shown by *stars*. The *single growth curve*, lower curve in the diagram, is based on $\mu = 7.192$ and $Th/U = 4.62$ with primordial $^{206}Pb/^{204}Pb$ and $^{207}Pb/^{204}Pb$ of 9.307 and 10.294, respectively (Tatsumoto et al. 1973) at 4.57 Ga. The *secondary growth curve* by Stacey and Kramers (1975), depicted with S-K, assumes separation of the secondary reservoir at 3.70 Ga, with $\mu = 9.735$ and $Th/U = 3.78$; note that isochrons of various ages (*dash-dotted lines*) are not relevant to the ages of mineralization

Linear arrays of Pb isotopic data may be interpreted as isochrons or mixing lines. In either case, the variations demonstrate that fluids containing different Pb isotopes were involved in vein formation. If the slopes define the ages of mineralization, Pb should have been leached from rocks of different $^{238}U/^{204}Pb$ (μ) and $^{232}Th/^{204}Pb$ (ω) by fluids and then precipitated in the veins at a given time. This hypothesis can be readily discounted because the data show different $^{207}Pb/^{206}Pb$ slopes. It is not feasible to form a steep $^{207}Pb/^{206}Pb$ slope for galena associated with Au, a less steep line for galena associated with Au at Ross, and a much more gentle slope for altaite at KL at a given geological time.

The second model involving a mixing of Pb from various sources may be further subdivided into two alternatives: radiogenic Pb may have been introduced into the veins (1) during the vein formation, or (2) significantly later. The latter possibility is rejected because isotopic exchange of galena/altaite with fluids involves dissolution and precipitation of the minerals. Galena and altaite are commonly intergrown with Au-bearing minerals and other base-metal sulphides. It appears impossible to replace Pb minerals without producing any petrographic evidence of such alteration. Also, there are no overgrowth textures in galena/altaite, and if the latter process took place, rims of galena/altaite grains would be more radiogenic than the cores, and later veinlets should contain more radiogenic Pb than earlier ones. However, lead associated with Au, which is texturally late, is less radiogenic than Pb not associated with Au in earlier veins.

The isotopic variations are thus attributed to the presence of vein fluids carrying Pb from different sources. This is consistent with textures of the deposits; the Au deposits commonly show non-equilibrium mineral assemblages and cross-cutting veinlets of different minerals.

Source of metals

Presence of common metal source. Many genetic models for Archaean Au deposits propose the derivation of metals including Au from a "common reservoir," such as the mantle (e.g. Rock and Groves 1988; Rock et al. 1989), or large volumes of lower crustal rocks during their granulitization (e.g. Cameron 1988; Fyon et al. 1989). Gold in rocks is present in sulphides. Most of Pb also occurs in sulphides, while a portion of Pb may reside in silicates. Therefore, source rocks for Au would also have contributed significant amounts of Pb to hydrothermal fluids. The sections below examine the alternative hypotheses of derivation of metals from granulites and from mantle, and the evidence from Pb-isotopic data.

Distinct differences in isotopic data reject the direct derivation of metals from "a common source," but it is still possible that a small portion of the metals could have originated from "a common source" and that an addition of upper crustal Pb could have been modified their isotopic compositions.

If there is such a "common source," the isotopic composition of the source should lie on the extrapolation of lines through the Ross and KL data; such lines intersect at the point where, $^{206}Pb/^{204}Pb$, $^{207}Pb/^{204}Pb$ and $^{208}Pb/^{204}Pb$ are 13.5, 14.6, and 33.6, respectively (Figs. 5 and 6). The model requires an addition of non-radiogenic Pb at Ross and an addition of radiogenic Pb at KL. Radiogenic Pb would be readily available in the upper crust at KL, where abundant alkalic and sedimentary rocks are present as the host rocks. In the case of Ross, addition of non-radiogenic Pb from sulphides in old igneous rocks is required. Considering similar geological settings of the two, it is unlikely.

Granulitization as the source. Recent seismic study shows continuous horizontal layering in the middle to lower

crust beneath the entire Abitibi belt due to shallow thrusting in late Archaean time (e.g. Green et al. 1990). The structure and rocks beneath Ross and KL are probably not significantly different. If auriferous fluids were generated during the granulitization of lower crust due to crustal thickening, the chemistry of the fluids would have been very similar, and the common fluid would be expected to have the isotopic composition of the intersection of the two lines defined from two deposits.

The model is discounted because fluids associated with granulitization of old crustal rocks would have been highly radiogenic. Recrystallization of silicate minerals during high-grade metamorphism would have expelled decay products that cannot substitute in the crystal structures of those silicate minerals. It may be argued that fluids leached metals only from sulphides or from ultramafic rocks, which would have been less radiogenic. Preferential leaching from ultramafic rocks during regional metamorphism is unlikely and Pb loss recorded in many zircons in highly metamorphosed rocks (e.g. Corfu 1987) indicates the release of radiogenic Pb during granulitization.

Furthermore, Gariépy and Allègre (1985) postulated the presence of ~3.0 Ga granitic rocks beneath the southern Abitibi greenstone belt. Fluids released from such rocks at 2.6 Ga would have been highly radiogenic.

Also, the linear data from the two deposits on the $^{208}Pb/^{206}Pb$ vs $^{207}Pb/^{206}Pb$ diagram (Fig. 3) suggest that the source had similar Th/U ratios, but different contents of Th and U. The diagram is not consistent with the derivation of Pb during granulitization because granulitization tends to fractionate U and Th.

Mantle source. The proposed model by Rock and Groves (1988) and Rock et al. (1989) suggests derivation of metals from mantle together with alkaline igneous rocks. Sr- and Nd-isotopic studies suggest that the area was underlain by depleted mantle at ~2.7 Ga, and that greenstone-forming mafic volcanic rocks and alkalic igneous rocks in the area were both derived from a depleted mantle source (Machado et al. 1986; Hattori and Hart 1991). Lead isotopic compositions of the depleted mantle may be approximated from the data from 2.7 Ga komatiites in the southern Abitibi Belt; isotopic data by Tilton (1983) and Brévart et al. (1986) show that the $^{206}Pb/^{204}Pb$ ratios range from 13.3 to 13.4 and the $^{207}Pb/^{204}Pb$ ratios range from 14.4 to 14.5 (Fig. 6). These values are close, but not on the line of extrapolation of the values for Ross and KL deposits, suggesting that mantle Pb was an unlikely source for the deposits; even if the values were on the line of extrapolation, the contribution of Pb from the mantle to the overall Pb would be small, especially for KL. If mantle Pb was involved for Archaean Au deposits, then more of a mantle-signature would be expected, considering the abundance of mantle-derived alkaline rocks in the area (Hattori and Hart 1990).

Local rocks as the metal source. Distinct Pb-isotopic compositions from the two deposits (Figs. 3–5) reflect different metal sources for the two, considering the similar ages of the mineralization. Hydrothermal activity for the KL deposits involved rocks with high μ and ω ratios.

The Ross deposit is essentially hosted in tholeiitic basalts, which have low U and Th contents. The isotopic compositions of Pb not associated with Au are approximately parallel to the Pb growth curves (Fig. 6). This is consistent with the derivation of Pb from local tholeiites of 2715 Ma. Lead isotopic compositions of the tholeiitic rocks would have evolved parallel to the growth curves of Pb, while sulphides in the rocks would have retained the original isotopic compositions. Mixing of Pb from sulphides and rocks could have produced the Pb isotopic pattern in the diagram.

The less radiogenic nature of Pb compared to the contemporaneous mantle Pb, which is mostly associated with Au, may be attributed to the contribution of Pb from older mafic and ultramafic rocks, which have low U/Pb ratios. Old mafic rocks (>2.8 Ga) beneath the area contained Pb, which was less radiogenic than 2.7 Ga mantle values. Thus, data from the Ross deposit can be interpreted as the mixing of Pb from local rocks and Pb from old source.

More radiogenic Pb from the KL deposits also appears to suggest the derivation of Pb from local rocks, which are alkaline to subalkaline intrusive rocks, shoshonitic volcanic rocks, and graywackes and conglomerates. The ratios of U/Pb and Th/Pb are erratic, but generally high. Twenty representative samples of the host intrusions contain 1 to 5 ppm U and 5 to 20 ppm Th (this study) and volcanic rocks contain U up to 15 ppm and Th (up to 54 ppm; Kerrich and Watson 1984). If we assume that the mineralization took place at ~2.6 Ga, as suggested from other Au deposits (e.g. Jamielita et al. 1990), the rocks would have acquired radiogenic Pb, which explains the high $^{207}Pb/^{204}Pb$ ratios from KL (Fig. 6). This explanation, however, is not satisfactory for highly radiogenic values with relatively low $^{207}Pb/^{204}Pb$ ratios (Fig. 6). There are two possible explanations for these highly radiogenic data points: (1) these altaite grains were not formed in the Archaean or (2) the Pb was derived from an unusual reservoir. The highly radiogenic values from the KL deposits overlap with the values for sulphides in ~2.7 Ga BIF in the Abitibi belt (Fig. 6). The highly radiogenic values from BIF are considered to be primary because essentially no U is present in the sulphides. This suggests that highly radiogenic Pb was available at shallow crustal levels in the Archaean. This highly radiogenic Pb at 2.7 Ga requires a Pb reservoir with low $^{207}Pb/^{204}Pb$ ratios. The presence of such unusual reservoir is also inferred from VSM and Ross data, as described above. The slope of VMS data from the southern Abitibi Greenstone Belt extends away from the values of the Stacey-Kramers (1975) Pb crustal evolution curve towards low $^{207}Pb/^{204}Pb$ (Fig. 6). Such a Pb reservoir would produce Pb with the observed isotopic compositions in KL at ~2.6 Ga.

Derivation of significant Pb from local rocks is consistent with Pb isotope data from many other Archaean deposits. Radiogenic Pb signatures are observed in many Au deposits hosted by old rocks. Examples include deposits in the Chibougamau camp in northern Abitibi

belt (Thorpe et al. 1984) and in the Norseman greenstone belt of Western Australia (Browning et al. 1987). The interpretation presented here is also consistent with Pb-isotope studies at the Dome mine by Moritz et al. (1990), who concluded that most Pb was derived from nearby porphyries.

Genetic model of gold mineralization

Derivation of significant amounts of Pb from local rocks suggests other constituent elements would also have been leached from local rocks during the extraction of Pb. This is consistent with the variations of vein mineralogy and geochemical signatures observed among Archaean Au deposits on camp-scale. For example, tourmaline is common in deposits in and near shale-rich sedimentary rocks (e.g. the Val d'Or camp), scheelite occurs in deposits hosted by felsic intrusions (e.g. Hollinger-McIntyre deposit, Timmins) and fuchsite in deposits in ultramafic rocks (e.g. Dome deposit). Boron, W and Cr are likely to have leached from local rocks in the immediate areas.

The proposed model, however, does not reject the derivation of CO_2-rich fluids by a common process, such as granutilization and mantle degassing. The relatively homogeneous C-isotopes and fluid chemistry of many deposits may support a common origin for the fluids (e.g. Burrows et al. 1986). The model simply proposes different origins for different constituents. Fluids responsible for Au deposits probably became auriferous through the interaction with rocks during their ascent to shallow crustal levels. Fluids that did not encounter Au-rich rocks, such as ultramafic rocks, probably remained barren. Numerous occurrences of barren quartz-carbonate veins along major shear deformation zones in greenstone belts appear to support this proposition. Barren veins near KL deposits were also formed from low-salinity CO_2 fluids at similar temperatures (W. Zhan and K. Hattori, unpublished data). These fluids had a capacity to dissolve Au during their ascent to shallower crustal levels, but they were barren. It appears to indicate that the barren nature of fluids was due to the Au-poor nature of rocks through which the fluid passed during their ascent: barren fluids simply did not encounter Au-rich rocks. Auriferous ore fluids were formed when the fluids encountered Au-rich rocks. Decoupling of sources of fluid and metals proposed for Archaean Au deposits in this paper is consistent with the findings from Phanerozoic vein Au deposits, where fluids (meteoric water), S and metals originated from different sources (e.g. Hattori and Sakai 1979).

Conclusions

1. Galena and altaite from the Ross and KL deposits show significant Pb-isotopic variations among grains. The isotopic heterogeneity reflects non-mixing of various fluids for vein formation. The findings are consistent with the microtextures of the deposits, such as cross-cutting veinlets with different mineral parageneses.
2. The Pb-isotopic signatures for vein-forming fluids for the Ross and KL deposits are different. Distinct differences in the isotopic compositions of the two deposits are attributed to the derivation of most metals from local rocks. Mafic-ultramafic host rocks contributed considerable amounts of metals to the veins at Ross mine and alkalic to subalkalic intrusions have supplied metals to the veins at KL. The data are consistent with the derivation of metals from the local rocks significantly later than their magmatism at ~2.6 Ga. Different isotopic signatures of the two deposits indicate that the constituent metals in the deposits were not supplied from a single common source, such as the mantle or granulites.
3. Lead-isotopic compositions of galena associated with Au at Ross are less radiogenic than the values of the 2.7 Ga mantle, but are similar to the values for Archaean VMS deposits in the area. These values may have been derived from sulphides in older mafic-ultramafic rocks, which possibly underlie in the area.
4. Lead associated with Au tend to be less radiogenic than Pb associated only with base metals. These data are consistent with the derivation of Au from sulphides or ultramafic rocks.
5. This study suggests multiple sources for Au mineralization. Most metals and other constituents were likely leached from the upper crustal rocks during the fluid ascent, although the fluids may have been generated in lower crust or in the mantle by a common process. The proposed model reconciles apparently conflicting lines of evidence from Archaean Au deposits, such as provinciality of mineralogy and geochemical signatures, and relatively uniform fluid inclusion and C-isotope data.
6. Very radiogenic Pb with low $^{207}Pb/^{204}Pb$ at KL requires either mineralization at a much later time (Proterozoic time) or a unusual source reservoir with very low $^{207}Pb/^{204}Pb$. The latter interpretation is preferred because there is no petrographic and mineralogical evidence indicating later isotopic modification and because the presence of such a Pb reservoir is inferred from the data of VMS and BIF.

Acknowledgements. The isotopic measurements were carried out during the author's 10-month stay at M.I.T., during sabbatical leave from the University of Ottawa. The author thanks Ken Burrhus and Nobumichi Shimizu for maintenance of the ion microprobe facility and their assistance during the use of the equipment, Graham Layne for allowing the author to use his computer program for data acquisition, Jurek Blusztajn for his assistance with the thermal ionization mass spectrometry of the standard, Robert Gait of the Royal Ontario Museum for donating the altaite specimen, R.I. Thorpe for a sample from the Ross deposit and providing isotopic values for the sample, George Nemcsok of Lac Minerals at Kirkland Lake and geologists at Ross mine for assisting the sample collections, and Edward Hearn for drafting one diagram. The comments and helpful suggestions by John Blenkinsop, Brian Cousens, Eion M. Cameron, J. Al Donaldson, Ulrich Knittel, Nobumichi Shimizu and anonymous reviewers are much appreciated.

References

Akande SO (1982) Mineralogy and genesis of three vein systems, Ross Mine, Holtyre, Ontario. In: Hodder RW, Petruk W (eds)

Geology of Canadian Gold Deposits. Can Inst Min Metal Sp vol 24:94–97
Bell K, Anglin CD, Franklin JM (1989) Sm-Nd and Rb-Sr isotope systematics of scheelites: possible implications for the age and genesis of vein-hosted gold deposits. Geology 17:500–504
Brévart O, Dupré B, Allègre CJ (1986) Lead-lead age of komatiitic lavas and limitations on the structure and evolution of the Precambrian mantle. Earth Planet Sci Lett 77:293–302
Browning P, Groves DI, Blockley JG, Rosman KJR (1987) Lead isotope constraints on the age and source of gold mineralization in the Archaean Yilgarn Block, Western Australia. Ecol Geol 82:971–986
Burrows DR, Wood PC, Spooner ETC (1986) Carbon isotope evidence of a magmatic origin for Archaean gold-quartz vein ore deposits. Nature 321:851–854
Cameron EM (1988) Archaean gold: relation to granulite formation and redox zoning in the crust. Geology 16:109–112
Cameron EM, Hattori K (1985) The Hemlo gold deposit, Ontario: a geochemical and isotopic study. Geochim Cosmochim Acta 49:2041–2050
Colvine AC (1989) An empirical model for the formation of Archaean gold deposits: products of final cratonization of the Superior Province, Canada. Econ Geol Monograph 6:37–53
Corfu F (1987) Inverse age stratification in the Archaean crust of the Superior Province: evidence for infra- and subcrustal accretion from high resolution U-Pb zircon and monazite ages. Precambrian Res 36:259–275
Corfu F, Krogh TE, Kwok YY, Jensen LS (1989) U-Pb zircon geochronology in the southwestern Abitibi greenstone belt, Superior Province. Can J Earth Sci 26:1747–1763
Corfu F, Jackson SL, Sutcliffe RH (1991) U-Pb ages and tectonic significance of late Archaean alkalic magmatism and nonmarine sedimentation: Trimiskaming Group, Southern Abitibi belt, Ontario. Can J Earth Sci 28:489–503
Deloule E, Gariépy C, Dupré B (1989) Metallogenesis of the Abitibi greenstone belt of Canada: a contribution from the analysis of trace lead in sulfide minerals. Can J Earth Sci 26:2529–2540
Doe BR, Stacey JS (1974) The application of lead isotopes to the problems of ore genesis and ore prospect evaluation: a review. Econ Geol 69:757–776
Dupré B, Arndt NT (1990) Pb isotopic compositions of Archaean komatiites and sulfides. Chem Geol 85:35–56
Feng R, Kerrich R (1991) Single zircon age constraints on the tectonic juxtaposition of the Archean Abitibi greenstone belt and Pontiac subprovince, Québec, Canada. Geochim Cosmochim Acta 55:3437–3441
Franklin JM, Roscoe SM, Loveridge WD, Sangster DF (1983) Lead isotope studies in Superior and Southern Provinces. Geol Surv Can Bull 351
Fyon JA, Troop G, Marmont S, Macdonald AJ (1989) Introduction of gold into Archaean crust, Superior Province, Ontario – coupling between mantle initiated magmatism and lower crustal maturation. Econ Geol Monograph 6:479–490
Gariépy C, Allègre CJ (1985) The lead isotope geochemistry and geochronology of late-kinematic intrusives from the Abitibi greenstone belt, and the implications for late Archaean crustal evolution. Geochim Cosmochim Acta 49:2371–2383
Green AG, Milkereit B, Mayrand LJ, Ludden JN, Hubert C, Jackson SL, Sutcliffe RH, West GF, Verpaelst P, Simard A (1990) Deep structure of an Archaean greenstone terrain. Nature 344:327–330
Hart SR, Shimizu N, Sverjensky DA (1983) Toward an ore fluid lead isotope "stratigraphy" for galenas from the Viburnum trend, SE Missouri. In: Kisvarsanyi G, Grant SK, Pratt WP, Koenig JW (eds) Proceedings of the International Conference on Mississippi Valley-Type Lead-Zinc Deposits. University of Missouri, Rolla Press, Rolla, pp 257–270
Hattori K (1989) Alkaline magmatism: evidence for the tectonic setting of gold mineralization in Archean Superior Province, Canada; Abstr 28th Int Geol Congress, vol 2, p 30
Hattori K, Hart SR (1990) Late Archaean alkaline magmatism in the Kirkland Lake gold camp: Isotopic and geochemical constraints. Robert F, Sheahan PA, Green SB (eds) Proceedings of the NUNA Conference on Greenstone Gold and Crustal Evolution. Geol Assoc of Canada, pp 163–165
Hattori K, Hodgson CJ (1990) Gold-related geology in the Kirkland Lake and Timmins camps. Geol Surv Can Open File 2160
Hattori K, Levesque G (1989) Hydrothermal activity in the Kirkland Lake Intrusive complex. Ont Geol Surv Misc Paper 143:59–67
Hattori K, Sakai H (1979) D/H ratios, origins and evolution of the ore-forming fluids for the Neogene veins and Kuroko deposits of Japan. Econ Geol 74:535–555
Hicks KD, Hattori K (1988) Magmatic-hydrothermal and wallrock alteration petrology at the Lake Shore gold deposit, Kirkland Lake, Ontario. Ont Geol Surv Misc Paper 140:192–204
Jamielita RA, Davis DW, Krogh TE (1990) U-Pb evidence for Abitibi gold mineralization postdating greenstone magmatism and metamorphism. Nature 346:831–834
Jolly WT (1974) Regional metamorphic zonation as an aid in the study of Archaean terrains, Abitibi region, Ontario. Can Mineral 12:499–508
Kerrich R, Watson GP (1984) The Macassa Mine Archean Lode gold deposit, Kirkland Lake, Ontario: geology, patterns of alteration and hydrothermal regimes. Econ Geol 79:1104–1130
Macfarlane AW (1989) Lead, sulfur and strontium isotopes in the Hualgayoc area, Peru and lead isotope provinces of the central Andes. Ph D thesis, Harvard University, Cambridge, Mass
Machado N, Brooks C, Hart SR (1986) Determination of initial $^{87}Sr/^{86}Sr$ and $^{143}Nd/^{144}Nd$ in primary minerals from mafic and ultramafic rocks: experimental procedure and implications for the isotopic characteristics of the Archaean mantle under the Abitibi greenstone belt, Canada. Geochim Cosmochim Acta 50:2335–2348
Masliwec A, York D, Kuybida P, Hall CM (1985) The dating of Ontario's gold deposits. Ont Geol Surv Misc Paper 127:223–228
McKibben MA, Eldridge CS (1990) Radical sulfur isotope zonation of pyrite accompanying boiling and epithermal gold deposition: a SHRIMP study of the Valles Caldera, New Mexico. Econ Geol 85:1917–1925
Moritz RP, Crocket JH, Dickin AP (1990) Source of lead in the gold-bearing quartz fuchsite vein at the Dome mine, Timmins area, Ontario, Canada. Miner Deposita 25:272–280
OGS-MERQ (1983) Lithostratigraphic map of the Abitibi Subprovince, Ontario Geological Survey-Ministère de l'Energie et des Ressources, Québec. 1:50,000, catalogued as Map 2148 in Ontario and DV83-16 in Québec
Ploeger FR, Crocket JH (1982) Relationship of gold to syenitic intrusive rocks in Kirkland Lake. In: Hodder RW, Petruk W (eds) Geology of Canadian Gold Deposits. Can Inst Min Metal Spec vol 24:69–72
Rock NMS, Groves DI (1988) Do lamprophyres carry gold as well as diamond. Nature 332:253–255
Rock NMS, Groves DI, Perring CS, Golding SD (1989) Gold, lamprophyres and porphyries: what does their association mean. Econ Geol Monograph 6:609–625
Schandl ES, Gorton MP (1991) Postore mobilization of rare earth elements at Kidd Creek and other Archaean massive sulfide deposits. Econ Geol 86:1546–1553
Sinclair WD (1982) Gold deposits of the Matachewan area, Ontario. In: Hodder RW, Petruk W (eds) Geology of Canadian Gold Deposits. Can Inst Min Metal Spec vol 24:83–93
Stacey JS, Kramers JD (1975) Approximation of terrestrial lead isotope evolution by a two-stage model. Earth Planet Sci Lett 26:207–221
Tatsumoto M, Knight RJ, Allègre CJ (1973) Time differences in the formation of meteorites as determined from the ratio of ^{207}Pb to ^{206}Pb. Science 180:1279–1283
Thomson JE, Charlewood GH, Griffin K, Hawley JE, Hopkins H, MacIntosh CG, Ogrizlo SP, Perry OS, Ward W (1950) Geol-

ogy of the main ore zone at Kirkland Lake. Ont Dep Mines Ann Rep 57:54–188

Thorpe RI (1982) Lead isotope evidence regarding Archaean and Proterozoic metallogeny in Canada. Rev Bras Geosci 12:510–521

Thorpe RI, Guha J, Franklin JM, Loveridge WD (1984) Use of the Superior Province lead isotope framework in interpreting mineralization stages in the Chibougamau district. In: Guha J, Chown EH (eds) Chibougamau stratigraphy and mineralization. Can Inst Min Metal Spec vol 34:496–516

Tilton GR (1983) Evolution of depleted mantle: the lead perspective. Geochim Cosmochim Acta 47:1191–1197

Tilton GR, Kwon ST (1990) Isotopic evidence for crust-mantle evolution with emphasis on the Canadian Shield. Chem Geol 83:149–163

Troop DG (1986) Multiple ore body types and vein morphologies, Ross Mine, District of Cochrane. Ont Geol Surv Misc Paper 132:413–420

Wong L, Davis DW, Krogh TE, Robert F (1991) U-Pb zircon and rutile geochronology of Archaean Greenstone formation and gold mineralization in the Val d'Or region, Quebec. Earth Planet Sci Lett 104:325–336

Editorial responsibility: J. Hoefs